JOURNAL OF MATERIALS SCIENCE 3 (1968) 61–69

The Influence of Boron Content on the Fine Microstructure of Pyrolytic Graphite

R. N. KATZ, C. P. GAZZARA
Ceramics Research Laboratory, Army Materials and Mechanics Research Center, Watertown, Massachusetts, USA

Received 1 September 1967

A study of the fine microstructure of boronated pyrolytic graphite was made utilising optical and X-ray diffraction techniques. The influence of boron content on the laminar structure, the lattice parameter, the lattice strain, the particle size, and the flexural strength of pyrolytic graphite was studied. Significant changes in the behaviour of all investigated parameters were observed in the 0.50 to 0.75 wt % boron range. A mechanism relating these changes to the appearance of a boron carbide deposit is hypothesised.

1. Introduction

It has been known that the nature of the growth cone structure of pyrolytic graphite bears a strong relationship to the mechanical properties [1, 2]. It is conceivable, however, that other microstructural features of a finer nature may also exert some influence on these properties. Such fine structural features include the laminar features revealed by mercury-ion bombardment etching [3], the X-ray crystallite size, the lattice parameter, and the magnitude of lattice strains. It is this finer scale microstructure which is investigated in this paper. The influence of boron content on the growth cone structure, the laminar features which are revealed by mercury-ion bombardment etching, the magnitude of X-ray strain broadening, the lattice parameter in the c direction, and the X-ray crystallite size will be shown. In addition, the above phenomena will be related to the variation with boron content of the flexural strength obtained from these materials. An hypothesis which relates the observed behaviour will be presented.

2. Materials and Test Procedures

The material used in this investigation was obtained from the Raytheon Company, Waltham, Massachusetts. Five plates of boronated pyrolytic graphite were deposited at 1850° C. The compositions (in wt %) of four of the plates were 0.25, 0.50, 0.75, and 1 % B and the fifth plate had a nearly linear compositional gradient along one direction ranging from approximately 1.2 to 3.3 % B. One plate of pyrolytic graphite deposited under the same conditions with 0 % B was also obtained as a control. For mechanical tests, bend specimens of dimension $2\frac{1}{2} \times \frac{3}{8} \times \frac{1}{4}$ in. (62.5 × 9.4 × 6.3 mm) were cut from each plate, the $\frac{1}{4}$ in. (6.3 mm) dimension corresponding to the c or growth direction. The specimens from the first four plates had compositions which were 0.25, 0.50, 0.75, and 1 % B respectively throughout the specimens. The bars taken from the fifth plate were cut so that they would give compositions of approximately 1.3, 2.3 and 3.3 % B in the middle of the $2\frac{1}{2}$ in. (62.5 mm) length of the bar. This insured that each bar cut from the fifth plate would have the same boron content in the portion of the bar which bears the maximum load during a 4-point loading flexural test. Therefore the flexural strengths obtained were representative of the compositions quoted. One can have confidence that the effects noted on the 1.3, 2.3 and 3.3 % B specimens are due to increasing boron content even though the actual boron content in the 2.3 and 3.3 % B specimens may have varied by as much as 0.25 % B. The density of all of the material, within the sensitivity of the measurements, was 2.21 to 2.22 g/cm^3 or 98.5 % of theoretical.

Mechanical tests were performed in 4-point loading with a 1 in. (25.0 mm) central span. Tests

were performed on an Instron Testing Machine with a 0.02 in. (0.5 mm)/sec strain rate. All testing was performed at room temperature. Reported flexural strengths are calculated from simple beam theory with no correction for shifting of the neutral axis. Five or six measurements were taken per datum point. In all cases the tension surface of the bars corresponded to the deposition surface of the pyrolytic material.

Metallographic specimens were cut from the same plates or areas of the plates as the bend specimens, polished, and observed under polarised light. Several bend specimens of each type were also polished and examined to insure that the microstructures of the samples selected for metallographic study were truly representative. The specimens subjected to mercury-ion bombardment cathodic etching [3] were first mechanically polished. They were then etched for 20 min with a 100 V driving potential between the specimen and earth.

The X-ray diffraction analysis of the boron-doped graphite specimens was made as follows.
(*a*) The solid samples were peeled on double adhesive tape resulting in a specimen less than $\frac{1}{64}$ in. (0.4 mm) thick to minimise reflecting aberrations. All specimens were taken $\frac{1}{4}$ in. (6.3 mm) along the *c* direction from the deposition surface.
(*b*) Automatic ratemeter chart recording of 2θ scans were made of the (00.2) and (00.4) reflections, using Ni-filtered CuKα radiation.
(*c*) The lattice constants of the samples, in the *c* direction, were computed using a least squares programme with an error function $\delta = \sin\theta \cos^2\theta$ [4] and a weighting factor of $1/\cos^2\theta$ [5]. The lattice constant of pure graphite, annealed at 3000° C for $\frac{1}{2}$ h, was determined by using this least squares analysis on the (00.2) Kα and (00.4) Kα reflections, as well as an analysis utilising the resolved peaks (00.4) Kα_1, (00.4) Kα_2, (00.6) Kα_1, (00.6) Kα_2, (00.2) Kβ, (00.4) Kβ, (00.2) Kα, and (00.6) Kβ. The two values of the lattice constant for pure graphite plus a consideration of the drift term in the analysis established the magnitude of the error of the lattice constant values.
(*d*) The X-ray diffraction peak breadths at half-maximum were used to compute the effective particle size of the samples in the *c* direction. The diffraction peak widths of the (00.2) and (00.4) reflections include a contribution from both the particle size and a distortion or strain effect. The effective particle size for these reflections, in the *c* direction, was computed after correcting for the separation of the Kα_1 and Kα_2 diffraction peaks and for instrumental broadening (using the pure graphite annealed at 3000° C for $\frac{1}{2}$ h as a standard [6]). An analysis of the particle size, in the *a* direction, using the (10.) X-ray diffraction peak, failed to indicate any conclusive relation between particle size, strain broadening, or lattice constant changes in the *a* direction, and changes in concentration of boron.

3. Results

3.1. Mechanical Properties

Fig. 1 shows the flexural strength of boron-doped pyrolytic graphite as a function of boron content. It will be noted that in going from 0 to 0.50% B the strength falls off, then from 0.75% B rapidly increases with boron content to about 1.3% B, continues to increase gradually to 2.3% B, and then falls slightly at 3.3% B. The uniformity of composition among specimens in the 1.3 to 2.3% B range was demonstrated by the small amount of scatter encountered.

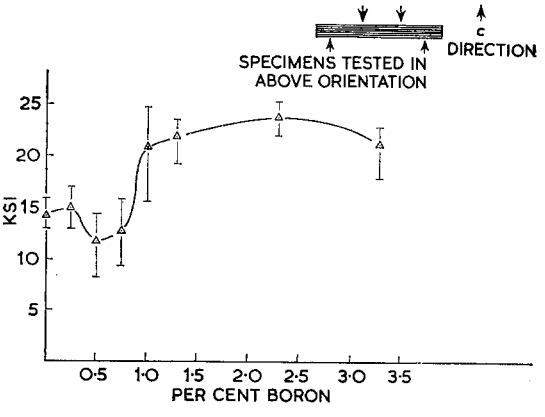

Figure 1 Graph of flexural strength of boronated pyrolytic graphite against wt % boron. *Note* ksi units are used in this diagram. 1 ksi = 1000 lb/in.^{2} = 0.7 kg/mm^2.

3.2. Optical Metallography

The structures observed in mechanically polished specimens viewed in polarised light at 100×, showed that all of the material is singularly nucleated coarse cone material. *No differences* in microstructure were uncovered by this technique. A typical microstructure is shown in fig. 2. By contrast, the laminar structure produced by mercury-ion bombardment, as viewed

at 500× under polarised light, revealed that considerable differences occur with increasing boron content.

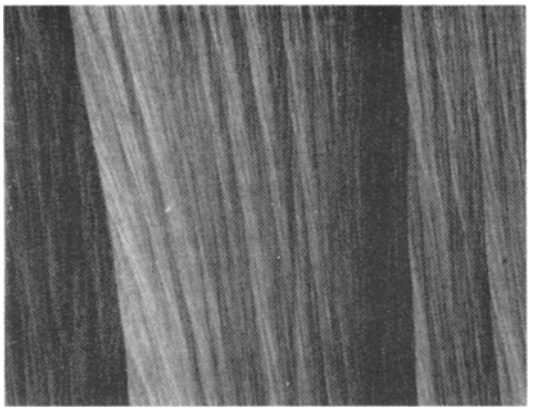

Figure 2 Singularly nucleated coarse cone structure of boronated pyrolytic graphite. Microstructure typical of graphites containing 0 to 3.3% B. (Polarised light, ×65).

Fig. 3a shows the nature of the laminar features typical of 0 to 0.5% B samples. Fig. 3b shows the structure of the 0.75% B samples. The size and distribution of these laminar features present in the compositions between 0 and 0.75% B were essentially the same, although some transition was evident at the 0.75% B composition. At a composition of 0.5% B, the more prominent laminar features were approximately 20 to 60 μm long and 2 to 3 μm thick, and they were continuous across the cone boundaries, as shown in fig. 3a. When the boron content changed to 1%, the laminar features decreased in length very markedly to about 10 to 20 μm and did not exceed 2 μm in width; these features have also lost, to a large degree, their continuity across the primary cone boundary, as shown in fig. 3c. At 1.3% B the laminar features were further reduced in size to the 5 to 15 μm range, and were only 1 μm thick; again there was a general lack of continuity across the boundary (fig. 3d). As the boron content was further increased to 2.3% B the same trend continued, as evidenced in fig. 3e. However, when the boron content reached 3.3% B, extremely long thick laminar features appeared throughout the structure. These features were longer and thicker than those in the 0.50% B material, and they were less closely spaced, as is shown in fig. 3f. Such features were also evident in one portion of a nominal 2.3% B sample. In this particular sample they were associated with a "band", similar to banding in alloy steels, which ran across the entire specimen. However, this "banding" was not a general feature in the 2.3% B sample, whereas the heavy laminar features were quite general in the 3.3% B sample.

3.3. X-ray Diffraction Analysis

The variation of the lattice constant in the c direction of the boron-doped pyrolytic graphite is presented in fig. 4. This variation in lattice parameter is consistent with the effects of boron content on the graphitisation of boronated pyrolytic graphites measured by Kotlensky [7], although the region of increase in c spacing is shifted to lower boron additions.

The procedure of Williamson and Hall [8] was followed for computing the root mean square strain $(\bar{\eta}^2)^{\frac{1}{2}}$, in the c direction. Large strain values having a Gaussian strain distribution were assumed where:

$$(\bar{\eta}^2)^{\frac{1}{2}} = \frac{\beta\cos\theta.c}{0.89\lambda l\sqrt{2\pi}} = \frac{\beta^*}{d^*\sqrt{2\pi}} = \frac{\epsilon}{\sqrt{2\pi}}$$

and: β is the corrected peak breadth; θ, the Bragg angle; c, the lattice constant; l, the Miller index; λ, the wavelength; 0.89 = shape constant [9]; $\beta^* = \beta\cos\theta/0.89\lambda$; $d^*_{00.l} = l/c$; ϵ is the slope of β^*/d^* curve for (00.2) and (00.4) peaks.†

Applying the equation to the (00.2) and (00.4) X-ray diffraction peaks, the maximum and minimum values of $(\bar{\eta}^2)^{\frac{1}{2}}$ computed for the boronated samples were 0.0072 and 0.0046 respectively. The maximum value of $(\bar{\eta}^2)^{\frac{1}{2}}$ is not as high as the value of 0.10 reported for thoria (obtained using a similar analysis procedure, [10]), but is considerably higher than values obtained for metals, i.e. $(\bar{\eta}^2)^{\frac{1}{2}} = 0.001$ for Al and W [8].

Figs. 5 and 6 show the results of refined calculations on this basis yielding the variation with boron content of strain and particle size (in absolute, not normalised, units), respectively, in the c direction. It can be seen from fig. 6 that the absolute particle size is a maximum for specimens containing approximately 0.75% B, and then slowly decreases to a level considerably

†The absolute particle size is taken from this curve as $1/\beta^*$ at $d^* = 0$.

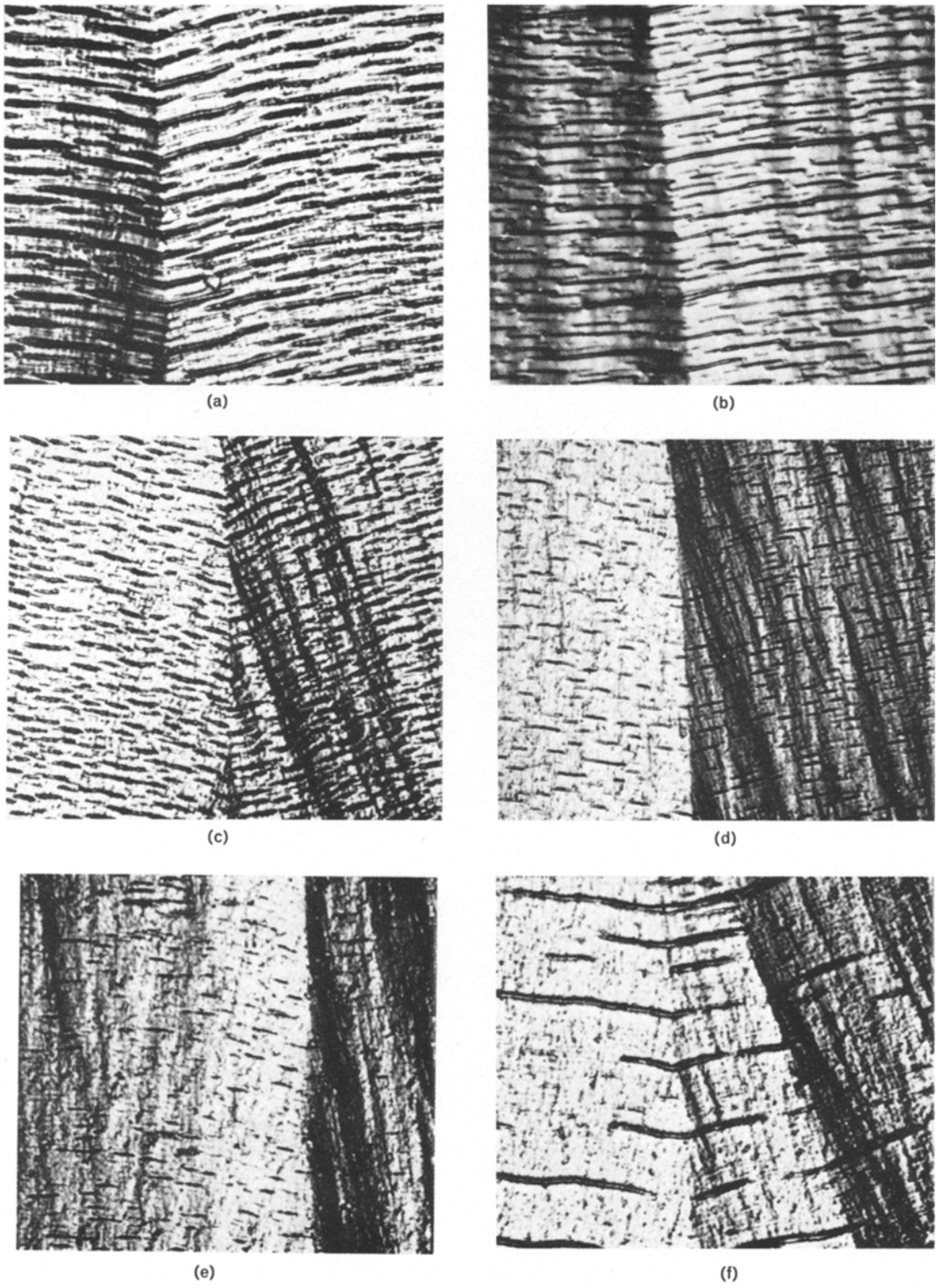

Figure 3 Laminar structure of boronated pyrolytic graphite revealed by mercury-ion bombardment etch; *c* direction ↑. (Polarised light, ×370). (a) 0.5% B; (b) 0.75% B; (c) 1% B; (d) 1.3% B; (e) 2.3% B; (f) 3.3% B.

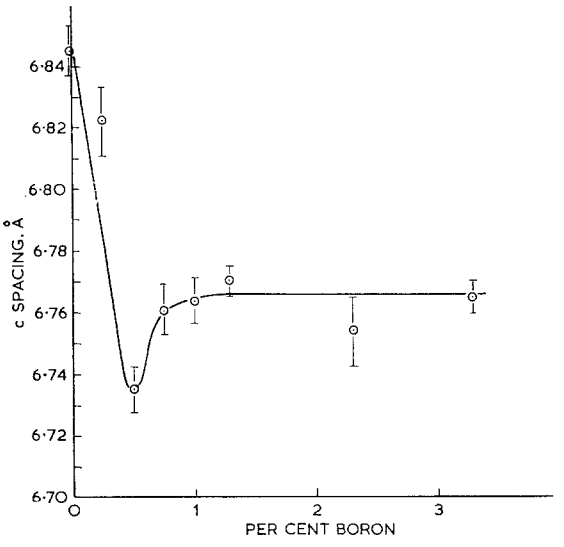

Figure 4 Graph of lattice parameter in the *c* direction against wt % boron.

above the pure graphite particle size value. The particle size for 0.50% B is given as two values differing from each other by more than the limits of error of the X-ray diffraction results. This was probably due to a slight difference in the boron content of the two specimens used to obtain the curve.

The error bars shown in figs. 5 and 6 were calculated on the basis of a 5% experimental error limit in the peak width of the (00.2) and the (00.4) reflections. It should be emphasised that the absolute values of particle size and strain are correct to the extent of the validity of the assumptions made, namely, the shape constant, the size and distribution functions of crystallite size and strain. The shapes of the curves drawn in figs. 5 and 6 are unchanged, however, regardless of the assumptions made, since no changes in the curves could be observed in changing from normalised to absolute units.

4. Discussion of Results

The results presented in the preceding section have indicated that the boron content exerts a large influence on the laminar features, the *c* lattice parameter, the X-ray strain broadening, the crystallite size, and the flexural strength. A coincidence of inflections in figs. 1, 4, 5 and 6 with respect to boron content is also quite apparent. Clearly some major change is occurring in this material as the composition changes from the 0.25 to 0.50% B region to the 0.75 to 1% B region. The problem of finding a mechanism which will explain the simultaneous occurrence of these seemingly diverse phenomena now presents itself.

Arai and Kanter [11] have observed that boron in graphite up to 4000 ppm is essentially in solid solution, although at 4000 ppm some may be present as B_4C. Lowell [12] has recently determined the boron/B_4C solvus line on the boron/carbon phase diagram. He found that the maxi-

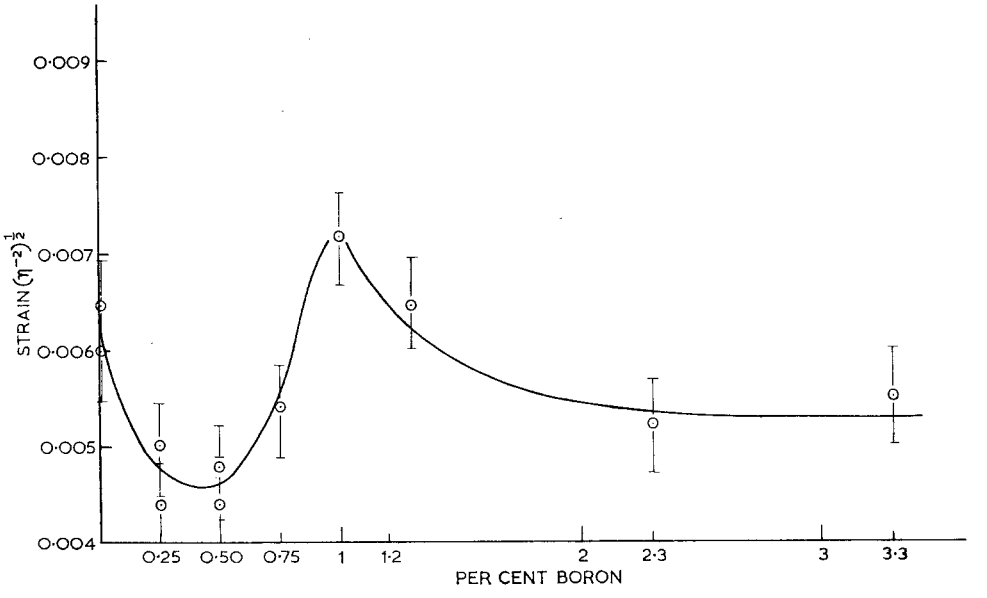

Figure 5 Graph of lattice strain in the *c* direction against wt % boron.

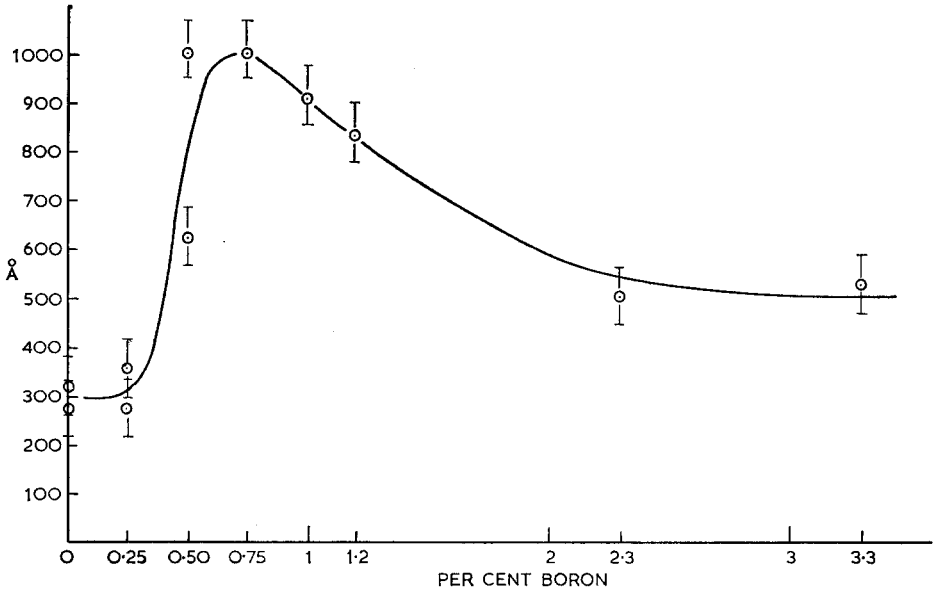

Figure 6 Graph of X-ray crystallite size in the *c* direction against wt % boron.

mum solubility of boron in natural graphite at 1850° C is approximately 1%, and that substitutional boron in the graphite decreased the lattice parameter. Kotlensky [7], for boronated pyrolytic graphite deposited at 2000° C, has also noted a reduction of lattice spacing with substitutional boron up to approximately 1%, after which the lattice parameter starts to increase, but within the compositions studied did not regain its original value. He attributes the increase to the presence of interstitial boron. This interstitial boron is most likely present as B_4C based on the findings of Arai and Kanter [11], and Lowell [12]. Thus, the variation in *c* spacing with boron content shown in fig. 4 is essentially in agreement with the findings of Kotlensky [7], namely that the substitutionally added boron (up to 0.5% B) enhances graphitisation (that is decreases the *c* spacing) and interstitial boron present as B_4C increases the *c* spacing. Owing to difference in deposition conditions and the nature of the graphites involved, one cannot be exact in stating the solubility limit of boron in the graphite tested in this investigation on the basis of the above-mentioned solubility studies. However, on the basis of all available evidence, the solubility limit must be between 0.4 and 1% – the very region in which large changes of behaviour were observed in the investigated parameters. It therefore seems likely that the results listed above are related to the appearance of B_4C.

The presence of B_4C can be used to explain both the appearance and disappearance of microstrains in the lattice, and the transitions noted above in the laminar features revealed by mercury-ion etching. If the B_4C deposits pyrolytically together with the carbon, it is possible that small regions of B_4C will form a coherent interface with the graphite lattice. Coherent interfaces are known to produce severe volume microstrains in the matrix [13]. As the boron concentration increases, it is likely that the size of B_4C deposits increases. If this were the case, eventually they would lose coherency, and become a second phase with a non-coherent boundary. Such a loss in coherency should be observable by a relief of the microstrains that were present because of the coherent boundary. The X-ray strain broadening behaviour indicates only small strains present at 0.50% B, severe strains present at 1 and 1.3% B, and small strains again at 2.3 and 3.3% B, and this variation can be understood in terms of no or very limited B_4C deposits present at 0.50% B, coherent deposits of B_4C present at 1 and 1.3% B, and non-coherent deposits present at 2.3 and 3.3% B.

The presence of B_4C deposits also provides a rationalisation for the behaviour of the laminar structure of the boronated pyrolytic graphite with increasing boron content. To understand how this results, no claim need be made for the exact nature of the microfeatures, other than to

state that they are truly boundaries between regions in the graphite, and not microcracks. That these features are not microcracks has been substantiated previously by electron microscopy [3, 4] and the deflection of such a laminar feature by a scratch, as shown in fig. 7, rather conclusively illustrates this point. Although these features are not themselves cracks, there are often microcracks associated with the features. This is shown in the electron micrograph in fig. 8. The features are present in the as-deposited material, and so must be a result of the deposition process. They are also present in material with 0% B and so can not be a second phase. If B_4C is depositing together with the pyrolytic graphite, it is possible that the B_4C deposits will limit the geometrical extent of the laminar features, i.e. the greater the amount of dispersed B_4C, the greater the restriction of the extent and boundary of the laminar features. This behaviour is observed in the composition range 0.50 to 2.3% B. The banding effect in the 3.3% material may result from favoured areas of deposition for B_4C, but the authors have no substantive evidence to validate this.

The process described above is analogous to a

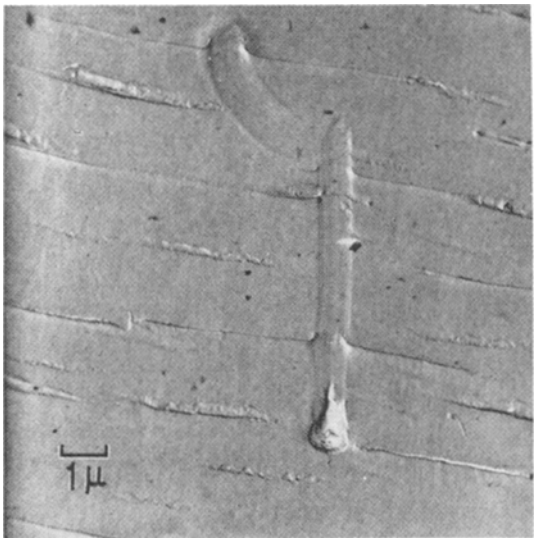

Figure 7 Scratch deflecting laminar features in 0.5% B sample. Cr-shadowed replica.

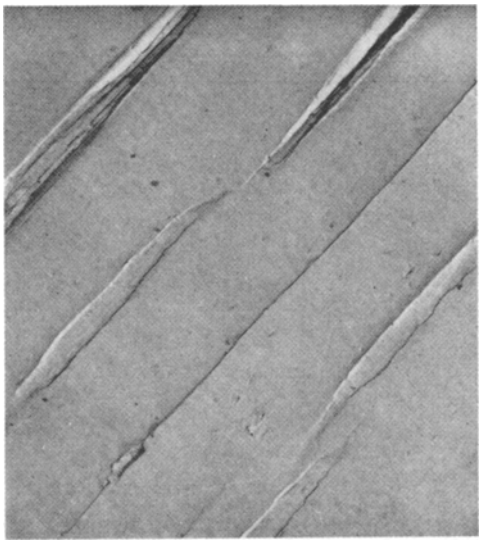

Figure 8 Microcracks associated with laminar features in pyrolytic graphite containing 0.5% B. Cr-shadowed replica (×6125).

coherent/non-coherent precipitation phenomenon typically encountered in age-hardened metals. On this basis, the improved flexural strengths in going from 0.50 to 2.3% B and the slight drop in strength in going to 3.3% B, can be understood. It is interesting to note that the presence of boron in excess of 0.50% inhibits the shear mode of failure. Most specimens of these compositions did not fracture, but rather lost their ability to carry a load. This resulted from the generation of one or more delaminations* perpendicular to the *c* axis of the specimen. The slight increase in the strength of the 0.25% B specimens as compared with the 0% specimens is probably a consequence of the lower magnitude of lattice strains in these specimens.

The microscopic, and X-ray diffraction, evidence cited in the preceding paragraphs indicates but does not conclusively prove the existence of the hypothesised B_4C dispersion hardening process. However, strong corroborative evidence for this process was obtained from the electron diffraction analysis of second phase particles extracted from a 2.3% B sample during replication for electron microscopy. These

*The distinction made in this paper between failures in the shear mode and delaminations is as follows. *Shear mode failures* are considered to be the typical fractures obtained in brittle materials, inclined at approximately 45° to the neutral plane of the specimen, whereas *delaminations* refer to a loss of cohesion, along the layers of graphite, which gives the specimen the appearance of one or more macrodislocations of the type originally described by Volterra [see A. H. Cottrell "Dislocations and Plastic Flow in Crystals" (Oxford University Press, Oxford, 1953) p. 32] lying parallel to the neutral plane

particles were principally located at the interface between the laminar features and the matrix, and were first observed at the 2.3% B level. One of the particles studied is indicated by the arrow in fig. 9; this particle is situated on the boundary of a large laminar feature and the matrix. The significance of observing a second phase at the 2.3% B level is that if the coherent/non-coherent B_4C deposit hypothesis is correct, then one would not expect to observe a second phase (by other than X-ray diffraction techniques) until the second phase becomes non-coherent, and this non-coherence would be predicted to occur between 1.3 and 2.3% B. Electron diffraction patterns of these particles were obtained, and a typical pattern is shown in fig. 10. An analysis of the spots in these patterns revealed that after eliminating the spots which could have been caused by the chromium shadowing and the graphite matrix, the patterns could have been produced by either rhombohedral boron or B_4C.

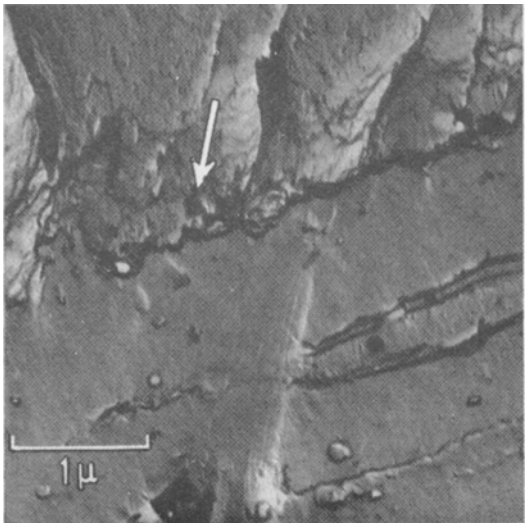

Figure 9 Electron micrograph of a pyrolytic graphite sample containing 2.3% B, showing second phase pull-out used for electron diffraction. Cr-shadowed replica.

Although the electron diffraction results cannot distinguish whether boron or B_4C is the second phase, a strong thermodynamic argument may be made for B_4C, since it has a negative free energy of formation at the deposition temperature [15]. Regardless of the exact second phase involved, its appearance at the

Figure 10 Electron diffraction pattern obtained from second phase particle.

composition predicted provides strong support for the hypothesis advanced here.

5. Summary

In this paper the authors have shown some of the effects of boron on the fine microstructure of pyrolytic graphite. It has been shown that the flexural strength of boronated pyrolytic graphite is related to the fine scale microstructural phenomena such as the laminar features and lattice strain, rather than the usually examined growth cone structure. A coherent/non-coherent boron carbide deposition mechanism was advanced to relate the observed results. Supporting evidence for this boron carbide deposition mechanism was obtained by electron diffraction studies performed on particles pulled out of the graphite matrix during replication.

Acknowledgement

The authors would like to express their thanks to Mr Maurice Dumais of the Army Materials and Mechanics Research Center for his aid in the electron microscopy.

References

1. R. N. DONADIO and J. PAPPIS, *Raytheon Tech. Memo* T-574 (1964).

2. J. J. GEBHART and J. M. BERRY, *American Institute of Aeronautics and Astronautics Journal* **3** (1965) 302.
3. A. TARPINIAN, *J. Amer. Ceram. Soc.* **47** (1964) 532.
4. H. P. KLUG and L. E. ALEXANDER, "X-ray Diffraction Procedures" (Wiley, New York, 1954).
5. J. B. HESS, *Acta Cryst.* **4** (1951) 209.
6. R. C. RAU, *Norelco Reporter* **10** (no. 3) (1963) 114.
7. W. V. KOTLENSKY, "The Effect of Boron on the Level of Graphitization of BPG", to be published in the Carbon Journal.
8. G. K. WILLIAMSON and W. H. HALL, *Acta Met.* **1** (1953) 22.
9. J. T. RANDALL, H. P. ROOKSBY, and B. S. COOPER, *Z. Krist.* **75** (1930) 196.
10. D. LEWIS and M. W. LINDLEY, *J. Nucl. Matls.* **17** (1965) 347.
11. G. J. ARAI and M. A. KANTER, Abstract 158, *Carbon* **5** (2) (1964) 400.
12. C. E. LOWELL, *J. Amer. Ceram. Soc.* **50** (1967) 142.
13. C. S. BARRETT and T. B. MASSALSKI, "Structure of Metals", 3rd edition (McGraw-Hill, New York, 1966).
14. R. N. KATZ and S. J. ACQUAVIVA, unpublished research, Army Materials and Mechanics Research Center.
15. C. E. WICKS and F. E. BLOCK, "Thermodynamic Properties of 65 Elements – Their Oxides, Halides, Carbides and Nitrides", *Bureau of Mines Bulletin* **605** (1963) 24.